ACS APPLIED MATERIALS & INTERFACES

Research Article

www.acsami.org

Selective Adsorption of Gd^{3+} on a Magnetically Retrievable Imprinted Chitosan/Carbon Nanotube Composite with High Capacity

Kai Li,[†] Qiang Gao,*[,†,‡] Gayatri Yadavalli,[§] Xiang Shen,[†] Hanwu Lei,[§] Bo Han,[†] Kaisheng Xia,[†] and Chenggang Zhou*[,†]

[†]Department of Chemistry, Faculty of Material Science and Chemistry and [‡]Engineering Research Center of Nano-Geo Materials of Ministry of Education, China University of Geosciences, Wuhan 430074, PR China

[§]Bioproducts, Sciences, and Engineering Laboratory, Department of Biological Systems Engineering, Washington State University, 2710 Crimson Way, Richland, Washington 99354-1671, United States

Supporting Information

ABSTRACT: A novel magnetic imprinting nanotechnology for selective capture of Gd^{3+} from a mixed solution of rare earth ions was developed by simply adding Gd^{3+}-imprinted chitosan/carbon nanotube nanocomposite (IIP-CS/CNT) and silica-coated magnetite nanoparticle (SiO_2@Fe_3O_4). The IIP-CS/CNT was prepared for the first time via a facile "surface deposition−crosslinking" method, exhibiting a well-defined coating structure. Interestingly, the neighboring IIP-CS/CNT monomers were held together as bundles, like a network, containing abundant interstitial spaces. When IIP-CS/CNT and SiO_2@Fe_3O_4 were dispersed in a mixed solution of rare earth ions, the magnetic SiO_2@Fe_3O_4 submicrospheres would be trapped in or adhere to the IIP-CS/CNT network, leading to the magnetization of IIP-CS/CNT; meanwhile, Gd^{3+} ions could be selectively captured by the magnetized IIP-CS/CNT. Saturation adsorption capacity for Gd^{3+} was up to 88 mg g^{-1} at 303.15 K, which is significantly higher than the Gd^{3+} adsorption capacities for the reported rare earth ion-imprinted adsorbents over recent years. The selectivity coefficients relative to La^{3+} and Ce^{3+} were 3.50 and 2.23, respectively, which are very similar to those found for other reported CS-based imprinted materials. Moreover, the imprinted adsorbents could be easily and rapidly retrieved by an external magnetic field without the need of additional centrifugation or filtration, greatly facilitating the separation process. Test of reusability demonstrated that the magnetized IIP-CS/CNT could be repeatedly used without any significant loss in binding capacity. Overall, this work not only provides new insights into the fabrication of magnetic imprinted CS-based composite, but also highlights its application for selective adsorption toward rare earth ions.

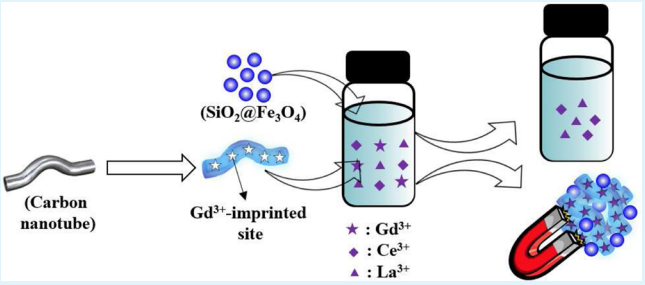

KEYWORDS: *Gd^{3+}, selective adsorption, imprinted nanocomposite, magnetically retrievable*

1. INTRODUCTION

Rare earth elements (REEs) with unique optical, electrical, and magnetic properties are considered strategically important for development of key technologies such as wind turbines, electrical car engines, medical diagnostics, and petroleum refining.[1] In recent years, with ever-increasing demand for high-purity REEs or their compounds, purification of individual REEs has received considerable attention.[2] However, such purification is particularly troublesome because REEs invariably co-occur together, and they have similar physical−chemical properties derived from their identical valence and similar ionic radii.[3] Several methods, including liquid−liquid extraction, chemical precipitation, ion exchange, and adsorption, have been widely used to separate REEs.[3,4] Among them, adsorption has been recognized as one of the most promising methods due to its simplicity, high efficiency, and wide-ranging availability.[5,6] The use of activated carbon, silica gel, and chelating resin as adsorbents of REEs has been repeatedly reported over recent decades.[7] However, these conventional adsorbents are usually limited by a lack of adsorption selectivity, although they might exhibit high adsorption capacity.[6]

Subsequently, much attention has recently been focused on the use of ion imprinted polymers (IIPs) for adsorption of REEs due to their special abilities to recognize a certain ion in terms of size.[3,8,9] General procedure for IIPs formation mainly consists of the preparation of a vinylated ligand−metal complex and its copolymerization with a cross-linker.[10] After removal of the templates (i.e., target metal ions), cavities will be formed inside polymer skeleton, which complement the templates in size and are capable of rebinding the templates selectively.[10] Although this approach has been widely used, a simpler method for preparation of IIPs is to directly cross-link the linear

Received: February 26, 2015
Accepted: September 10, 2015
Published: September 10, 2015

DOI: 10.1021/acsami.5b07560
ACS Appl. Mater. Interfaces 2015, 7, 21047−21055

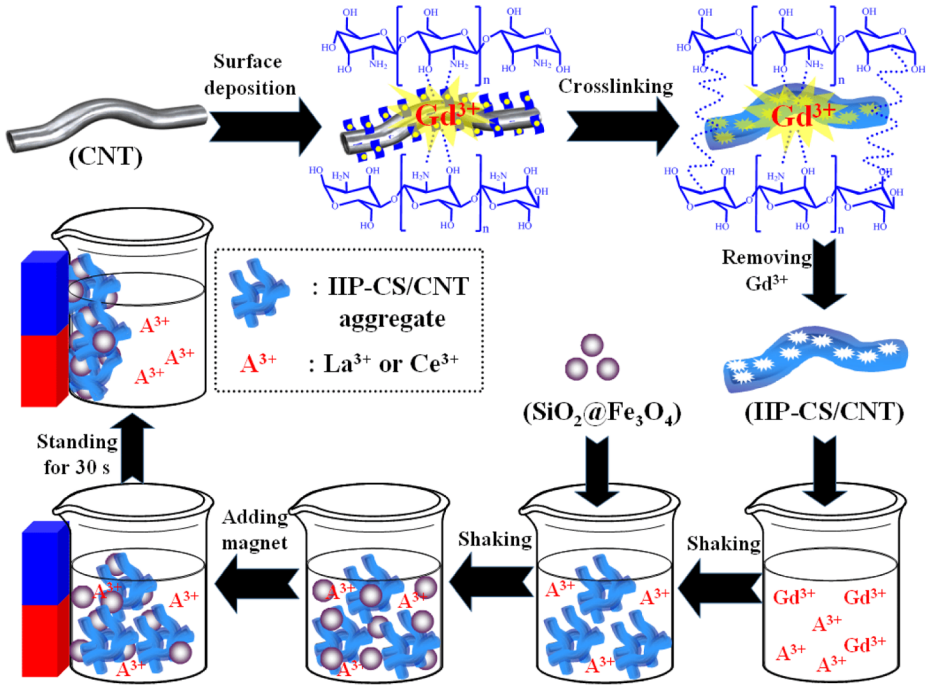

Figure 1. Preparation of magnetically retriveable IIP-CS/CNT and its application for selective adsorption of Gd^{3+}.

polymers that carry metal-binding groups. In such case, no radical polymerization is required, and the cross-linking step can be readily completed by a simple condensation reaction between linear polymer and bifunctional reagent (e.g., glutaraldehyde or epichlorohydrin).[10] Among various optional linear polymers, chitosan (CS) is the most popular one due to its impressive advantages of low cost, nontoxicity, abundant metal-coordinatable sites ($-NH_2$ and $-OH$), and easiness in being cross-linked.[11] However, it should be also noted that almost all the reported pure CS-based IIPs were processed into μm- or even mm-sized beads to facilitate their separation processes after adsorption.[12] Thus, template ions could hardly be removed completely. Moreover, poor accessibility to the recognition sites also made it difficult for target ions to rebind.[11]

Immobilizing imprinted CS on the surface of a high-surface-area nanomaterial seems to be a possible solution to overcome the previously-mentioned difficulties. This means that imprinted sites will be located at or close to solid surface, largely facilitating the diffusion of target ions to binding sites. Moreover, mechanical strength of imprinted CS can also markedly be enhanced.[13] Nevertheless, such CS-based imprinted nanocomposites have rarely been reported to date, mainly because their preparation is less straightforward and requires specially adapted protocols, and they have an inherent drawback of inconvenient separation from adsorption solution.[14] Therefore, it is highly desired to explore new possibilities for facile fabrication of CS-based imprinted nanocomposite and further to develop a method capable of isolating such imprinted nanoadsorbent conveniently.

Fortunately, recent research on the formation of non-imprinted CS-coated nanomaterials may provide a valuable rational guide for design of CS-based imprinted nanocomposites. Creative work was done by Liu's group,[15] in which they coated CS on carbon nanotube (CNT) via a simple "surface deposition−crosslinking" method, which takes advantage of the completely different solubility of CS in acidic (soluble) and basic (insoluble) solutions as well as the cross-linking reaction of surface-deposited CS with glutaraldehyde.[15] However, until now, no attempt has been made to combine imprinted CS with CNT by using a similar procedure, perhaps because the construction of imprinted CS on CNT is more complicated and especially because the existence of template ions probably disturbs the processes of surface deposition and cross-linking of CS. On the other hand, in our latest work, we prepared a CS/CNT composite via the "surface deposition−crosslinking" method and used it as a dye adsorbent for wastewater purification.[16] Interestingly, the CS/CNT could be magnetized by simply blending it with magnetic nanoparticles in aqueous solution ("blending" method). The phenomenon was based on the fact that CS/CNT monomers have a tendency to hold together as bundles in aqueous solution, and magnetic nanoparticles can be trapped in or adhere to these CS/CNT aggregates, leading to the formation of magnetic CS/CNT nanocomposite.[16]

Therefore, the objectives of this work are to (1) fabricate a novel Gd^{3+}-imprinted CS-coated CNT (IIP@CNT) nanocomposite by a modified "surface deposition−crosslinking" strategy; (2) make an attempt to magnetize IIP@CNT via the "blending" method; and (3) examine the performance of the magnetically retrievable IIP@CNT for selective adsorption of Gd^{3+} ion (Figure 1). A primary reason for selecting Gd^{3+} as the target ion is due to the fact that it is a representative of the most valuable REEs. For example, the permanent magnet prepared with addition of gadolinium can be used in room temperature magnetic refrigeration.[17] Gadolinium as a metal or salt has exceptionally high absorption capacity toward neutrons and therefore is used for shielding in nuclear reactors.[18] Gadolinium-containing contrast agent (addition of gadolinium complex) can significantly enhance the resolution of magnetic resonance imaging.[19,20] To reveal the adsorption properties of magnetically retrievable IIP-CS/CNT toward Gd^{3+}, effects of various operational parameters such as solution pH, contact time, temperature, and initial Gd^{3+} concentration on the

DOI: 10.1021/acsami.5b07560
ACS Appl. Mater. Interfaces 2015, 7, 21047−21055

adsorption efficiency were studied systematically. Furthermore, adsorption kinetics, adsorption equilibrium, adsorption selectivity (relative to La^{3+} and Ce^{3+}), and reusability of magnetically retrievable IIP@CNT were also investigated and discussed in detail.

2. MATERIALS AND METHODS

2.1. Synthesis of SiO_2@Fe_3O_4, IIP-CS/CNT, and NIP-CS/CNT. The information on chemicals used in this work can be seen in Text S1.

Silica-coated magnetite (SiO_2@Fe_3O_4) nanoparticles were prepared by a two-step strategy. First, magnetite (Fe_3O_4) nanoparticles were prepared via a hydrothermal process. Typically, 5.4 g of $FeCl_3 \cdot 6H_2O$ was dissolved in 160 mL of EG under magnetic stirring. Then, 14.4 g of NaAc and 4.0 g of PEG were added. After stirring for 0.5 h, the resultant solution was transferred into a Teflon lined stainless-steel autoclave with capacity of 200 mL. The autoclave was sealed, heated at 200 °C for 24 h, and then cooled to room temperature. The resultant solid product (Fe_3O_4) was collected with the help of a magnet, followed by washing with a recycle of ethanol and water several times, and finally dried in vacuum at 60 °C for 8 h. Second, magnetic Fe_3O_4 coated with silica (SiO_2@Fe_3O_4) was synthesized through a Stöber method with some modification.[21] Briefly, 120 mg of Fe_3O_4 was homogeneously dispersed in a mixture of ethanol (467 mL), water (139 mL), and ammonia solution (15 mL). Under continuous mechanical stirring, 6.0 mL of TEOS was slowly added to this dispersion. After stirring for 8 h at room temperature, silica layer was formed on Fe_3O_4 surface through hydrolysis and condensation processes. Finally, the resultant SiO_2@Fe_3O_4 particles were collected with the help of a magnet, washed with ethanol and water several times, and then dried in vacuum at 60 °C for 8 h. In our preliminary experiments, it was confirmed that the SiO_2 shell of SiO_2@Fe_3O_4 could effectively prevent the Fe_3O_4 core from leaching and further oxidation under harsh conditions (e.g., 1 mol L^{-1} HCl solution).

A composite of Gd^{3+}-imprinted chitosan and carbon nanotube (IIP-CS/CNT) was prepared via a modified "surface deposition−crosslinking" strategy (Figure 1): 1.0 g of $Gd(NO_3)_3 \cdot 6H_2O$ was first dissovled in 1000 mL of CS solution (1.0 g of CS was dissolved in 1000 mL of 2% (*v*/*v*) HAc solution), and the resultant solution was stirred vigorously for 2 h to reach an equilibrium of Gd^{3+} complex with CS. Then, 1.0 g of CNT was added. After being ultrasonically treated for 15 min, the mixture was stirred vigorously for another 1 h to facilitate dispersion of CNT. Afterward, 0.1 mol L^{-1} NaOH solution was added drop-wise into the mixture to adjust the pH value up to 7, with the aim of depositing the Gd^{3+}−CS complex onto CNT surface. Thereafter, the mixture was heated to 60 °C, and 0.5 mL of GA was introduced for crosslinking of Gd^{3+}−CS. The cross-linking principle is shown in Scheme S1. The Gd^{3+}-imprinted CS/CNT was collected by filtration and washed with diluted HAc (pH 4) to remove the adsorbed and excessive or uncross-linked CS. Finally, the Gd^{3+} ions imprinted in the adsorbent were removed by eluting with 1 mol L^{-1} HCl three times. The obtained material, that is, IIP-CS/CNT, was finally dried at 60 °C overnight.

The preparation procedure of nonimprinted CS-coated carbon nanotube (NIP-CS/CNT) was essentially similar to that of IIP-CS/CNT, except without the addition of Gd^{3+}.

The information about the characterization of materials involved in this work can be seen in Text S2.

2.2. Magnetization of IIP-CS/CNT and Batch Adsorption Procedures. Typically, 10 mg of IIP-CS/CNT and 30 mg of SiO_2@Fe_3O_4 were mixed with 20 mL of aqueous solution containing a precisely known Gd^{3+} concentration in a vial. Then, the vial was shaken in a thermostated shaker with a speed of 240 rpm. Once the adsorption reached equilibrium, the Gd^{3+}-adsorbed mIIP-CS/CNT was collected by application of an external magnet. Initial and equilibrium concentrations of Gd^{3+} were analyzed spectrophotometrically by taking an aliquot of 10 mL and adjusting the pH to 7.2 ± 0.1.

On the basis of a similar procedure described earlier, the effect of solution pH on adsorption efficiency was investigated with the initial Gd^{3+} concentration of 10 mg L^{-1} over the pH range from 2−7 at 303.15 K. The desired pH of Gd^{3+} solution was adjusted using 0.1 mol L^{-1} HCl or 0.1 mol L^{-1} NaOH solution.

Kinetic experiments were carried out at 303.15 K by varying contact time from 3−480 min at three different initial concentrations (10, 50, and 100 mg L^{-1}). Equilibrium adsorption isotherm experiments were conducted at three different temperatures (293.15, 303.15, and 313.15 K) over a range of initial Gd^{3+} concentrations from 2−200 mg L^{-1}. In our preliminary experiment, it was confirmed that no precipitate was formed when applied a maximum concentration of 200 mg L^{-1} in our experimental conditions.

The experimental details about selectivity recognition and reusability of mIIP-CS/CNT can been seen in Texts S3 and S4.

3. RESULTS AND DISCUSSION

3.1. Characterization of Materials. The physical−chemical characterization of adsorbent is crucial to prove that it is well developed. Thus, different techniques have been used to examine and validate the morphologies, compositions, and textures of the materials involved in this work.

3.1.1. SEM Images. For a morphological characterization of the samples, a field-emission scanning electron microscope (SEM) was used. The SEM images of Fe_3O_4, SiO_2@Fe_3O_4, CNT, IIP-CS/CNT, and mIIP-CS/CNT are presented in Figure 2. Clearly, Fe_3O_4 is made up of monodisperse and

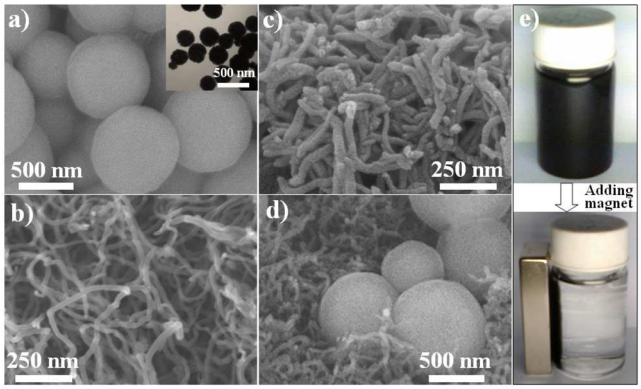

Figure 2. SEM images of (a) SiO_2@Fe_3O_4, (b) CNT, (c) IIP-CS/CNT, and (d) mIIP-CS/CNT (inset shows a TEM image of Fe_3O_4); (g) photographs of mIIP-CS/CNT solution before (above) and after (below) magnetic separation.

sphere-like nanoparticles with mean size of 250−300 nm (Figure 2a). It can be also found that SiO_2@Fe_3O_4 has a spherical morphology and smooth surface, with size ranging from 500−780 nm (Figure 2a). These results indicate that Fe_3O_4 nanoparticles have been expectedly prepared via a facile hydrothermal process, and coating of Fe_3O_4 with SiO_2 is also successfully achieved by the well-known Stöber method.[21] SEM images of CNT and IIP-CS/CNT are shown in Figure 2, panels b and c, respectively. It was observed that the CNT sample consists of nanotubes with diameters of about 28 nm and lengths of several micrometers (Figure 2b). Compared with CNT, IIP-CS/CNT retains a nanotube morphology and shows an obviously larger diameter (i.e., ca. 48 nm), confirming that CNT has been coated successfully with imprinted CS via the modified "surface deposition−crosslinking" method (Figure 2c). Moreover, no free CNT or CS particles but only uniform IIP-CS/CNT nanotubes can be observed, indicating that the imprinted CS polymers have been entirely deposited on the surfaces of CNT monomers to form well-defined coating layers.

DOI: 10.1021/acsami.5b07560
ACS Appl. Mater. Interfaces 2015, 7, 21047−21055

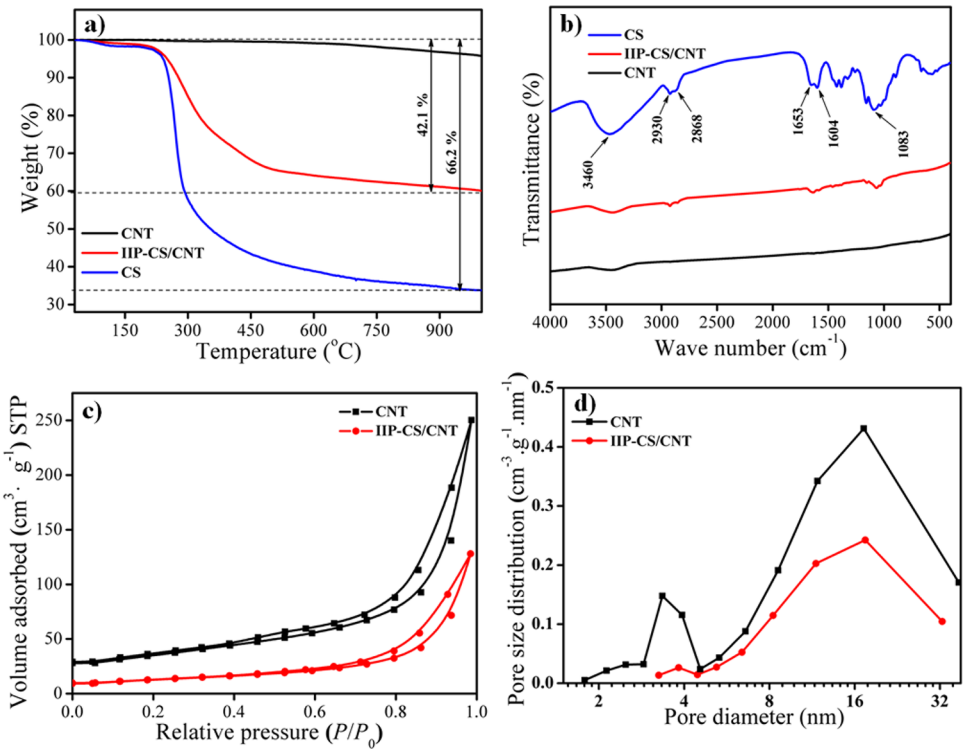

Figure 3. (a) TG curves of CNT, CS, and IIP-CS/CNT; (b) FT-IR spectra of CS, CNT, and IIP-CS/CNT; (c) N_2 adsorption−desorption of CNT and IIP-CS/CNT; and (d) pore size distribution of CNT and IIP-CS/CNT.

Interestingly, it was also found that the neighboring monomers of either CNT or IIP-CS/CNT sample form aggregated bundles, like a network, containing abundant interstitial spaces (Figure 2b,c). In our previous works,[22] we found that CNT bundles could be magnetized by blending them with magnetic nanoparticles in aqueous solution. Such magnetization of CNT was similar to a fishing process with a fishing net, where the fish were the magnetic nanoparticles, and the fishing net was composited of carbon nanotubes that were self-assembled together to form a network. When an external magnetic field was applied, the magnetic nanoparticles were trapped in or adhered to the CNT network, leading to the magnetization of CNT. Using the same strategy, we recently also realized the magnetization of CS/CNT.[16] Encouraged by these findings, we make an attempt in this paper to magnetize the IIP-CS@CNT via the "blending" strategy. As expected, the SiO_2@Fe_3O_4 could indeed be trapped in or adhere to the IIP-CS/CNT aggregate by introducing SiO_2@Fe_3O_4 into the IIP-CS@CNT dispersion solution followed by adding an external magnetic field (Figure 2d). The method was reliable, that is, all the IIP-CS/CNT nanoparticles can be magnetically retrieved (Figure 2e).

3.1.2. Thermogravimetric Analysis (TGA). To obtain the information about the imprinted CS layer on CNT, TGA measurement was conducted under the inert atmosphere (N_2 protection). The TGA curves of CNT, CS, and IIP-CS/CNT are shown in Figure 3, panel a. The weight of CNT remains essentially constant when the temperature is increased from 30 to 400 °C, and shows a slight decrease when the temperature further increases from 400 to 1000 °C. A possible reason accounting for this phenomenon is as follows: CNT has some defects on its surface including topological defects, rehybridization defects, and incomplete bonding defects.[23] These defects aid oxygen dissociation and result in C−O bond formation.[23] Upon heating to high temperatures (i.e., 400 to 1000 °C), these oxygen-containing groups will gradually vanish.

As for the samples of CS and IIP-CS/CNT, their weight losses below 200 °C should be due to the desorption of physically adsorbed water, and those between 280 and 450 °C should be ascribed to the degradation and deacetylation of CS.[16,24,25] An additional weight loss occurs at higher temperatures and should be due to the further condensation of carbonaceous surface species.[16] When heated to 1000 °C, the amount of solid residue of IIP-CS/CNT left is about 33.8 wt %, indicating that the content of CS in IIP-CS/CNT is considerably high.

3.1.3. Fourier Transform Infrared (FT-IR) Spectra. FT-IR spectroscopy was used to confirm grafting of IIP-CS in to the surface of CNT. Figure 3, panel b shows the FT-IR spectra of CS, CNT, and IIP-CS/CNT. The spectrum of CNT does not exhibit visible peaks in the range of 4000−400 cm^{-1}. By contrast, CS shows distinctive adsorption peaks at about 3460 cm^{-1} (the stretching vibration of $-NH_2$ and −OH), about 2930 and 2868 cm^{-1} (assigned to the stretching vibration of −CH, $-CH_2$, and $-CH_3$), 1604 cm^{-1} (the bending vibration of −NH in $-NH_2$), 1653 cm^{-1} (the stretching vibration of C═O in N-acetyl groups), and 1083 cm^{-1} (the stretching vibration of the C−O−C bridge), respectively.[16] Obviously, all these adsorption peaks also appear in the FT-IR spectrum of IIP-CS/CNT. This observation suggests that the imprinted CS layer was successfully formed on the surface of CNT, giving rise to the IIP-CS/CNT nanocomposite.

3.1.4. N_2 Adsorption−Desorption Isotherms. To analyze and quantify pore structures and surface areas of CNT and IIP-CS/CNT samples, N_2 adsorption−desorption isotherms were determined, and the results are shown in Figure 3, panel c. Both CNT and IIP-CS/CNT show a type II isotherm with a big H3 hysteresis loop in the P/P_0 ranges of 0.4−1.0 and 0.65−1.0,

DOI: 10.1021/acsami.5b07560
ACS Appl. Mater. Interfaces 2015, 7, 21047−21055

respctively.[26] The H3 hysteresis loop is usually given by aggregates of adsorbents containing slit shaped pores.[26] Pore size distributions of the CNT and IIP-CS/CNT samples, calculated via BJH method based on desorption curves, are presented in Figure 3, panel d. The peak centered at about 3.5 nm corresponds to the inner cavities of nanotubes,[16] while the distribution extending from 4.5 to 32 nm should be attributed to the secondary pores resulting from aggregates of nanotubes. Because of the existence of imprinted CS, the IIP-CS/CNT shows lower surface area and pore volume (44.8 $m^2\ g^{-1}$; 0.20 $cm^3\ g^{-1}$) than pure CNT (121.7 $m^2\ g^{-1}$; 0.39 $cm^3\ g^{-1}$).

3.2. Adsorption Studies. The wide applications of Gd increase the demand for developing an advanced process to recover such REE in high purity.[17−19] However, it is currently difficult to separate Gd^{3+} from aqueous samples containing other rare earth ions such as La^{3+} and Ce^{3+} because of their same identical valence (trivalent) and similar hydrated ionic radii (r_{Gd3+} = 0.938 Å, r_{La3+} = 1.061 Å, r_{Ce3+} = 1.034 Å).[27,28] Recent studies have demonstrated that imprinted polymers had great potential for selective adsorption of rare earth ions due to their special abilities to recognize a certain ion in terms of size.[3,8,9] However, simple but efficient design and fabrication of Gd^{3+}-imprinted materials with highly accessible binding sites and capability of being easily recovered still remains a challenge. In the present study, we successfully developed a facile way to obtain Gd^{3+}-imprinted nanoadsorbent (i.e., IIP-CS/CNT), based on a previous report for the preparation of CS-coated CNT,[15] and further confirmed that the IIP-CS/CNT could be magnetically retrieved by blending it with SiO_2@Fe_3O_4 in aqueous solution. Therefore, we speculated that the magnetically retrievable IIP-CS/CNT nanocomposite should have great potential for being used as a highly efficient adsorbent in selective adsorption of Gd^{3+}. To confirm this, the adsorption properties of magnetically retrievable IIP-CS/CNT toward Gd^{3+} were systematically investigated including pH effect, adsorption equilibrium, adsorption kinetics, adsorption selectivity (relative to La^{3+} and Ce^{3+}), and reusability.

3.2.1. Influence of pH on Adsorption Efficiency. The effect of the solution pH on the adsorption efficiency was investigated primarily since pH is one of the most important parameters that might influence adsorption capacity (Figure 4). In view of the fact that Gd^{3+} would form insoluble precipitate of $Gd(OH)_3$ in basic aqueous solutions, the pH values studied were performed over the range from 2−7. Figure 4 shows the adsorption capacity of mIIP-CS/CNT as a function of solution pH. Clearly, the adsorption capacity of mIIP-CS/CNT toward Gd^{3+} shows an obvious increase with the increase in the pH value. Since the Gd^{3+} adsorption took place via coordination interactions between Gd^{3+} ions and amino groups of CS, under acidic conditions, the protonation of these amino groups could reduce their binding abilities involved in chelating with Gd^{3+}. Hence, pH 7 was chosen as the optimal pH in the following experiments.

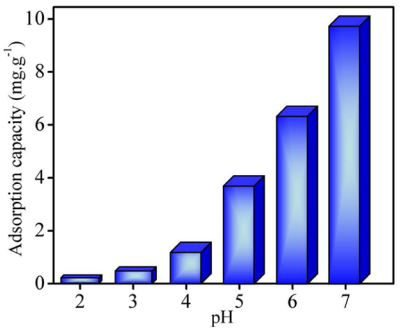

Figure 4. Effect of pH on the adsorption efficiency of Gd^{3+} onto mIIP-CS/CNT.

3.2.2. Adsorption Capacity and Rate. To figure out the adsorption capacity, the isothermal experiments of Gd^{3+} adsorptions onto mIIP-CS/CNT and mNIP-CS/CNT were performed, and the results are shown in Figure 5, panels a and b. For the Gd^{3+} adsorption onto mIIP-CS/CNT, it was found that the increase in adsorption temperature leads to an increase in adsorption efficiency. The maximum adsorption capacities of mIIP-CS/CNT toward Gd^{3+} at 293.15, 303.15, and 313.15 K are 68, 88, and 104 mg g^{-1}, respectively (Figure 5a). Such positive correlation between adsorption capacity and temperature can be also found in the literature.[29−31] To understand this phenomenon deeply, a thermodynamic analysis was conducted.[32,33] The values of Gibb's free energy change (ΔG^0), enthalpy change (ΔH^0), and entropy change (ΔS^0) were listed in Table 1. The negative values of ΔG^0 (−21.6 to −23.6 kJ mol^{-1}) confirm the feasibility of the process and spontaneous adsorption of Gd^{3+} on mIIP-CS/CNT.[32] Moreover, the increase in negative value of ΔG^0 with the increase in temperature indicates that the adsorption process becomes more favorable at higher temperatures.[32] A positive value of ΔH^0 (9.0 kJ mol^{-1}) suggests that the interaction of Gd^{3+} adsorbed by mIIP-CS/CNT is endothermic in nature, which also explains why the adsorption capacity of mIIP-CS/CNT toward Gd^{3+} ions increases with the increase in temperature.[29−31] From Table 1, it can be also found that the ΔS^0 has a value of 104.3 J $mol^{-1}\ K^{-1}$, which suggests the randomness at the solid−solution interface in the adsorption system increases during the adsorption process. The positive ΔS^0 value may be due to the release of water molecule produced by complexation between the Gd^{3+} ions and the functional groups on the surfaces of mIIP-CS/CNT.[34]

Furthermore, the analysis of isotherm data by fitting them to different isotherm models was conducted to find the suitable model that could accurately depict the adsorption processes (Figure 5).[35,36] The predicted isotherms by nonlinear analyses of Langmuir and Freundlich models for the adsorptions of Gd^{3+} onto mIIP-CS/CNT at three different temperatures (293.15, 303.15, and 313.15 K), and the adsorptions of Gd^{3+} onto the imprinted (i.e., mIIP-CS/CNT) and nonimprinted (i.e., mNIP-CS/CNT) materials at 303.15 K are shown in Figure 5, panels a and b, respectively. Clearly, in call cases, the Langmuir model provides best fits to the experimental data. Table 2 summarizes the fitted parameters (q_m, K_L, K_F, and $1/n$) of these isotherm models and the corresponding correlation coefficients (R^2). Through a comparison between R^2 values of three isotherms, Langmuir model is also found to be the best one that can describe the equilibrium data satisfactorily. The results indicate that the binding sites of mIIP-CS/CNT and mNIP-CS/CNT are uniformly distributed on their surfaces, and the adsorption of Gd^{3+} are regarded as monolayer adsorption.

At a given temperature (i.e., 303.15 K), it can be also found that the mIIP-CS/CNT has higher adsorption capacity than the control mNIP-CS/CNT at all concentration ranges, confirming the effectiveness of the ion imprinting (Figure 5).

To clarify the adsorption rate, kinetic experiments of Gd^{3+} adsorption onto mIIP-CS/CNT and mNIP-CS/CNT were also conducted, and the results are shown in Figure 6, panels a and

DOI: 10.1021/acsami.5b07560
ACS Appl. Mater. Interfaces 2015, 7, 21047−21055

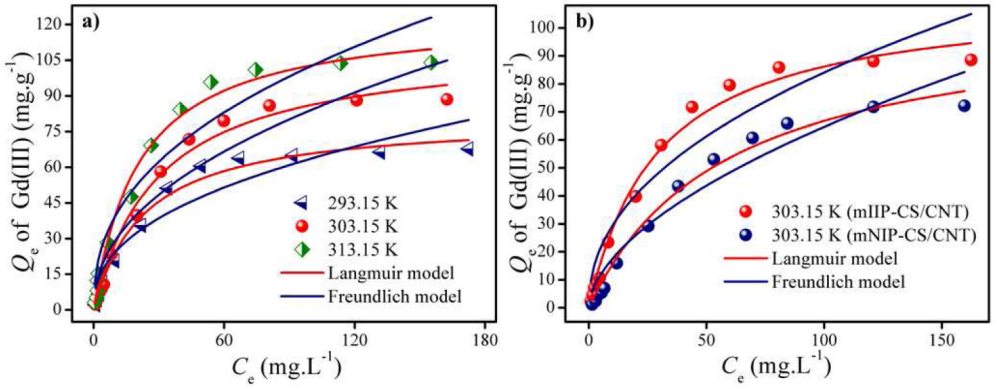

Figure 5. (a) Adsorption isotherm data of Gd^{3+} onto mIIP-CS/CNT at 293.15, 303.15, and 313.15 K, and (b) the isotherm data of Gd^{3+} adsorptions onto mIIP-CS/CNT and mNIP-CS/CNT at 303.15 K.

Table 1. Thermodynamic Parameters for the Adsorption of Gd^{3+} Adsorptions onto mIIP-CS/CNT

T (K)	ΔG^0 (kJ mol^{-1})[a]	ΔH^0 (kJ mol^{-1})[b]	ΔS^0 (J mol^{-1} K^{-1})[b]
293.15	−21.6	9.0	104.3
303.15	−22.5		
313.15	−23.6		

[a]ΔG^0 was calculated by the following equations: $\Delta G^0 = -RT \ln K_0$, and $K_0 = (C_{ad,e}/C_e)$, where $C_{ad,e}$ is the amount of Gd^{3+} adsorbed on the adsorbent per liter of the solution at equilibrium, and C_e is the equilibrium concentration of Gd^{3+} in solution. [b]ΔH^0 and ΔS^0 were calculated by the following equation: $\Delta G^0 = \Delta H^0 - T\Delta S^0$.

b. In each case, the adsorption capacity significantly increases during the initial stage and then slowly reaches equilibrium within 120 min. This phenomenon may be explained as follows: during the adsorption process, the adsorption on the exterior surface would first reach saturation, and then Gd^{3+} ions took a relatively longer contact time to diffuse into the pores of adsorbent to achieve equilibrium.[32]

Nonlinear fittings of adsorption data with pseudo-first-order and pseudo-second-order kinetic models for the adsorptions of Gd^{3+} onto mIIP-CS/CNT at three different initial concentrations (10, 50, and 100 mg L^{-1}), and the adsorption of Gd^{3+} onto mNIP-CS/CNT at 10 mg L^{-1}, are shown in Figure 6, panels a and b, respectively.[37] The calculated values of kinetic parameters (k_1, k_2, $q_{e,calc,1}$, and $q_{e,calc,2}$) and the corresponding correlation coefficients (R^2) are presented in Table 3. Compared with the pseudo-first-order model ($0.9503 < R^2 < 0.9811$), the pseudo-second-order model fitted the experimental data well, with higher correlation coefficients ($0.9899 < R^2 < 0.9993$). Moreover, the adsorption capacities predicted by pseudo-second-order model ($q_{e,calc,2}$) well agree with the results obtained experimentally ($q_{e,exp}$), which also suggests the suitability of pseudo-second-order model. This also means that the adsorption rate is proportional to the square of the number of free sites, which corresponds to the term $(q_e - q_t)^2$ in the pseudo-second-order model.[38]

3.2.3. Selectivity Study. La^{3+} and Ce^{3+} were chosen as competitive metal ions because the two rare earth ions and Gd^{3+} had identical valences and similar ion radii. Table 4 summarizes the K_d, k, and k' values of La^{3+} and Ce^{3+} with repect to Gd^{3+}. When they coexisted in the same medium, a competition would start for the same binding sites of mIIP-CS/CNT. The Gd^{3+} adsorption capacity of mIIP-CS/CNT was found to be much higher than those for La^{3+} and Ce^{3+} ions. The relative selectivity coefficient (k') is an indicator to express an adsorption affinity of recognition sites to target ions. From Table 4, it can be seen that the k' values of mIIP-CS/CNT for Gd^{3+}/La^{3+} and Gd^{3+}/Ce^{3+} are 3.50- and 2.23-times greater than those of mNIP-CS/CNT, respectively. Considering the facts that the radius of Gd^{3+} is pretty close to those of La^{3+} and Ce^{3+}[39] and the selectivity of imprinted adsorbent for the target ions (i.e., Gd^{3+}) is simply determined by the ion geometry, it can be concluded that the Gd^{3+} ions can be selectively adsorbed even in the presence of interferences of some competitive metal ions.

3.2.4. Comparison with Other Similar Type of Adsorbents. To further assess the adsorption selectivity of mIIP-CS/CNT, a comparison between mIIP-CS/CNT and other reported CS-

Table 2. Adsorption Isotherm Constants for Gd^{3+} Adsorptions onto mIIP-CS/CNT and mNIP-CS/CNT

		temperature (K)			
		293.15	303.15	313.15	303.15
isotherm model	model parameter	mIIP-CS/CNT			mNIP-CS/CNT
Langmuir[a]	q_m (mg g^{-1})	79.48	109.3	121.51	96.52
	K_L (L mg^{-1})	0.0440	0.0367	0.0559	0.0214
	R^2	0.9942	0.9919	0.9954	0.9840
Freundlich[b]	K_F (mg$^{1-1/n}$ L$^{1/n}$ g^{-1})	9.320	10.72	16.31	5.55
	$1/n$	0.4140	0.4470	0.4004	0.5288
	R^2	0.9248	0.9197	0.9231	0.9229

[a]Langmuir model is expressed as $q_e = ((q_m K_L C_e)/(1 + K_L C_e))$, where C_e is the equilibrium concentration of Gd^{3+}, q_e and q_m are the amount of Gd^{3+} adsorbed at equilibrium and the maximum adsorption capacity, respectively, and K_L is the Langmuir binding constant. [b]Freundlich model is expressed as follows: $q_e = K_F C_e^{1/n}$, where K_F and $1/n$ are Freundlich constants, respectively.

DOI: 10.1021/acsami.5b07560
ACS Appl. Mater. Interfaces 2015, 7, 21047−21055

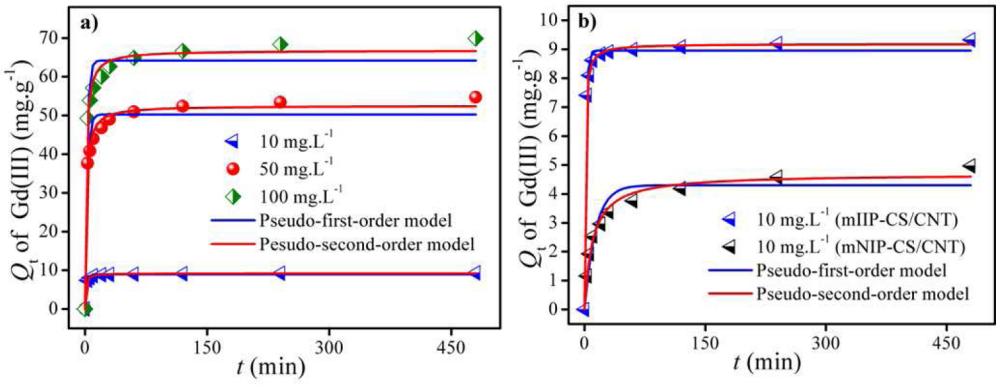

Figure 6. (a) Adsorption kinetic data of Gd^{3+} onto mIIP-CS/CNT at initial concetrations of 10, 50, and 100 mg L^{-1}, and (b) kinetic data of Gd^{3+} adsorptions onto mIIP-CS/CNT and mNIP-CS/CNT at 10 mg L^{-1}.

Table 3. Kinetic Parameters for Gd^{3+} Adsorptions onto mIIP-CS/CNT and mNIP-CS/CNT

		initial concentration (mg L^{-1})			
		10	50	100	10
kinetic model[a]	model parameter	mIIP-CS/CNT			mNIP-CS/CNT
pseudo-first-order model	$q_{e,exp}$ (mg g^{-1})	9.329	54.72	69.89	4.967
	k_1 (min^{-1})	0.5405	0.3705	0.4073	0.0740
	$q_{e,calc,1}$ (mg g^{-1})	8.959	50.26	64.18	4.299
	R^2	0.9911	0.9553	0.9604	0.9350
pseudo-second-order model	k_2 (g mg^{-1} min^{-1})	0.1467	0.0128	0.0110	0.0210
	$q_{e,calc,2}$ (mg g^{-1})	9.190	52.50	66.82	4.690
	R^2	0.9993	0.9899	0.9905	0.9841

[a]Pseudo-first-order and pseudo-second-order kinetic models are expressed as $q_t = q_e(1 - e^{-k_1 t})$ and $q_t = ((k_2 q_e^2 t)/(1 + k_2 q_e t))$, respectively, where q_e and q_t are the adsorption capacities at equilibrium and at time t, respectively; k_1 and k_2 are the equilibrium rate constants of pseudo-first-order and pesudo-second-order models, respectively.

Table 4. K_d, k, and k' Values of La^{3+} and Ce^{3+} with Respect to Gd^{3+}

	mIIP-CS/CNT		mNIP-CS/CNT		
metal ion	K_d (mL g^{-1})	k	K_d (mL g^{-1})	k	k'
Gd^{3+}	1813.85		751.53		
La^{3+}	472.33	3.84	685.33	1.097	3.50
Ce^{3+}	941.16	1.93	870.69	0.863	2.23

based imprinted adsorbents was conducted, and the k' values are presented in Table 5.[14,40−44] It can be found that our values of k' (Gd^{3+}/La^{3+}, 3.50; Gd^{3+}/Ce^{3+}, 2.23) are consistent with the reported results, indicating that the adsorption selectivity of mIIP-CS/CNT is satisfactory.

Adsorption capacity is another important factor to evaluate an imprinted adsorbent. As shown in Figure 5, panel a, the maximum adsorption capacity of mIIP-CS/CNT was found to be 104 mg g^{-1} at 313.15 K. Taking into account the fact that the adsorption of rare earth ions, in practice, is generally performed at room temperature, we used the adsorption capacity value 88 mg g^{-1} at 303.15 K to compare with the Gd^{3+} adsorption capacities for the reported rare earth ion-imprinted adsorbents over recent years (Table 6).[3,9,45−47] Nevertheless, it is obvious that the adsorption capacity of mIIP-CS/CNT (88 mg g^{-1}) is much higher than those of materials prepared by other imprint techniques. Moreover, compared with other reported rare earth ion-imprinted absorbents, the mIIP-CS/CNT has an obvious advantage that it can be easily and rapidly retrieved by an external magnetic field without the need of additional centrifugation or filtration, greatly facilitating the separation process (Figure 2e).

Table 5. Comparison of Relative Selectivity Coefficients (k') between the CS-Based Imprinted Adsorbents

CS-based imprinted adsorbent	target ion	completive ion	relative selectivity coefficient (k')	ref
magnetic Cu(II) ion imprinted composite	Cu^{2+}	Ni^{2+}	2.66	14
mesoporous silica SBA-15-supported Pb(II)-imprinted polymer	Pb^{2+}	Hg^{2+}	2.21	40
magnetic Cu(II) ion Imprinted composite	Cu^{2+}	Co^{2+}	2.32	41
Ce(III)-imprinted polymer supported by mesoporous SBA-15 matrix	Ce^{3+}	Fe^{3+}	3.2	42
dithiocarbamate modified chitosan beads	Pb^{2+}	Cu^{2+}	2.45	43
imprinted CS hydrogels	Ag^{+}	Cu^{2+}	3.75	44
magnetically retriveable IIP-CS/CNT	Gd^{3+}	La^{3+}	3.50	this work
magnetically retriveable IIP-CS/CNT	Gd^{3+}	Ce^{3+}	2.23	this work

Table 6. Comparison of Binding Capacities between the Rare Earth Ion-Imprinted Adsorbents

rare earth ion-imprinted adsorbent	imprinted rare earth ion	binding capacity (mg g^{-1})	ref
imprinted styrene−divinylbenzene copolymer	Dy^{3+}	40.15	9
ionic imprinted resins based on EDTA and DTPA derivatives	Gd^{3+}	24.53	45
IIP-HQP/SiO_2	Pr^{3+}	18.32	3
Sc(III) ion-imprinted polymers	Sc^{3+}	12.8	46
Lu(III) IIP	Lu^{3+}	64.2	47
magnetically retriveable IIP-CS/CNT	Gd^{3+}	88	this work

3.2.5. Reusability of Adsorbent. From pracital application of view, reusability is a crucial factor for an advanced adsorbent. Thus, we attempted to reuse the exhausted mIIP-CS/CNT

DOI: 10.1021/acsami.5b07560
ACS Appl. Mater. Interfaces 2015, 7, 21047−21055

after its regeneration by eluting with 1 mol L^{-1} HCl solution. The results of five consecutive adsorption−desorption cycles are shown in Figure 7. It can be found that the adsorption

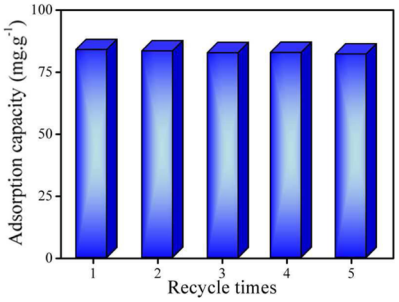

Figure 7. Results of five consecutive adsorption−desorption cycles with initial Gd^{3+} concentration of 200 mg L^{-1}.

capacity of the recycled mIIP-CS/CNT keeps relatively constant (88 to 86 mg g^{-1}) in five consecutive cycles. This result indicates that the mNIP-CS/CNT is reusable.

For a nanoadsorbent-based adsorption system, one of the most frequently encountered problems is that a certain amount of adsorbent nanoparticles will be lost during the adsorption or desorption processes. As a result, the adsorption capacity will gradually decrease. Thanks to magnetic retrievability, the mIIP-CS/CNT could be collected from aqueous solution without any significant weight loss and thus showed nearly invariable adsorption capacity cycle by cycle. This result indicates that mIIP-CS/CNT can be used as a cost-efficient adsorbent for selective adsorption of Gd^{3+}.

4. CONCLUSION

A novel ion imprinted nanocomposite IIP-CS/CNT, with a well-defined coating structure, was successfully prepared via a facile "surface deposition−crosslinking" process. When IIP-CS/CNT and SiO_2@Fe_3O_4 were dispersed in Gd^{3+} solution, the SiO_2@Fe_3O_4 could be trapped in or adhere to the IIP-CS/CNT aggregates, leading to the magnetization of IIP-CS/CNT; meanwhile, the Gd^{3+} was selectively captured by the magnetized IIP-CS/CNT. The amount of Gd^{3+} adsorbed was found to vary with solution pH, contact time, and initial Gd^{3+} concentration. The best pH value for favorable Gd^{3+} adsorption is 7. The adsorption equilibrium was achieved within 120 min, and the maximum adsorption capacity obtained was up to 88 mg g^{-1} at 303.15 K. Isotherm modeling revealed that the Langmuir equation well described the adsorption of Gd^{3+} onto magnetically retrievable IIP-CS/CNT. Fitting of kinetic data confirmed that the pseudo-second-order model provided the best correlation with the experimental data. The selectivity coefficients relative to La^{3+} and Ce^{3+} were 3.50 and 2.23, respectively, which are very similar to those found for other reported CS-based imprinted materials. Compared with other reported rare earth ion-imprinted absorbents, the magnetically retrievable IIP-CS/CNT not only had obviously high adsorption efficiency, but also could be easily manipulated by an external magnetic field. A test of reusability demonstrated that the magnetically retrievable IIP-CS/CNT could be repeatedly used without any significant loss in binding affinity. These unique features present the magnetically retrievable IIP-CS/CNT as a novel, promising, and feasible adsorbent applicable to selective adsorption of Gd^{3+}.

■ ASSOCIATED CONTENT

Supporting Information

The Supporting Information is available free of charge on the ACS Publications website at DOI: 10.1021/acsami.5b07560.

Summary of chemicals used; methods for material characterization; selectivity recognition experiment; study on reusability of adsorbent; cross-linking principle and process of Gd^{3+}-imprinted chitosan (PDF)

■ AUTHOR INFORMATION

Corresponding Authors

*E-mail: gaoqiang@cug.edu.cn. Phone: +86 027 6788 3731. Fax: +86 027 6788 3731.
*E-mail: cgzhou@cug.edu.cn.

Notes

The authors declare no competing financial interest.

■ ACKNOWLEDGMENTS

The authors acknowledge the research grants provided by the Fundamental Research Funds for the Central Universities, China University of Geosciences (Wuhan) (No. CUG120115), Special Fund for Basic Scientific Research of Central Colleges, China University of Geosciences (Wuhan) (No. CUGL090305), Land Resources Geology Survey Projects of China (Grant No. 12120113015300), and National Natural Science Foundation of China (Grant No. 21303170).

■ REFERENCES

(1) Kulaksız, K.; Bau, M. Anthropogenic Dissolved and Colloid/Nanoparticle-bound Samarium, Lanthanum and Gadolinium in the Rhine River and the Impending Destruction of the Natural Rare Earth Element Distribution in Rivers. *Earth Planet. Sci. Lett.* **2013**, *362*, 43−50.
(2) Jia, Q.; Tong, S. S.; Li, Z. Y.; Zhou, W. H.; Li, H. F.; Meng, S. L. Solvent Extraction of Rare Earth Elements with Mixtures of Sec-octylphenoxy Acetic Acid and Bis(2,4,4-trimethylpentyl) Dithiophosphinic Acid. *Sep. Purif. Technol.* **2009**, *64*, 345−350.
(3) Gao, B. J.; Zhang, Y. Q.; Xu, Y. Study on Recognition and Separation of Rare Earth Ions at Picometre Scale by Using Efficient Ion-surface Imprinted Polymer Materials. *Hydrometallurgy* **2014**, *150*, 83−91.
(4) Ogata, T.; Narita, H.; Tanaka, M. Adsorption Behavior of Rare Earth Elements on Silica Gel Modified with Diglycol Amic Acid. *Hydrometallurgy* **2015**, *152*, 178−182.
(5) Li, C. R.; Zhuang, Z. Y.; Huang, F.; Wu, Z. C.; Hong, Y. P.; Lin, Z. Recycling Rare Earth Elements from Industrial Wastewater with Flowerlike Nano-$Mg(OH)_2$. *ACS Appl. Mater. Interfaces* **2013**, *5*, 9719−9725.
(6) Sun, Y. B.; Shao, D. D.; Chen, C. L.; Yang, S. B.; Wang, X. K. Highly Efficient Enrichment of Radionuclides on Graphene Oxide-supported Polyaniline. *Environ. Sci. Technol.* **2013**, *47*, 9904−9910.
(7) Wang, F. C.; Zhao, J. M.; Zhou, H. C.; Li, W. S.; Sui, N.; Liu, H. Z. O-carboxymethyl Chitosan Entrapped by Silica: Preparation and Adsorption Behaviour toward Neodymium (III) Ions. *J. Chem. Technol. Biotechnol.* **2013**, *88*, 317−325.
(8) Alizadeh, T.; Amjadi, S. Synthesis of Nano-sized Eu^{3+}-Imprinted Polymer and Its Application for Indirect Voltammetric Determination of Europium. *Talanta* **2013**, *106*, 431−439.
(9) Biju, V. M.; Gladis, J. M.; Rao, T. P. Ion Imprinted Polymer Particles: Synthesis, Characterization and Dysprosium Ion Uptake Properties Suitable for Analytical Applications. *Anal. Chim. Acta* **2003**, *478*, 43−51.
(10) Branger, C.; Meouche, W.; Margaillan, A. Recent Advances on Ion-imprinted Polymers. *React. Funct. Polym.* **2013**, *73*, 859−875.

DOI: 10.1021/acsami.5b07560
ACS Appl. Mater. Interfaces 2015, 7, 21047−21055

(11) Guibal, E. Interactions of Metal Ions with Chitosan-based Sorbents: a Review. *Sep. Purif. Technol.* **2004**, *38*, 43−74.
(12) He, J.; Lu, Y. C.; Luo, G. S. Ca(II) Imprinted Chitosan Microspheres: An Effective and Green Adsorbent for the Removal of Cu(II), Cd(II) and Pb(II) from Aqueous Solutions. *Chem. Eng. J.* **2014**, *244*, 202−208.
(13) Chatterjee, S.; Lee, M. W.; Woo, S. H. Enhanced Mechanical Strength of Chitosan Hydrogel Beads by Impregnation with Carbon Nanotubes. *Carbon* **2009**, *47*, 2933−2936.
(14) Ren, Y. M.; Wei, X. Z.; Zhang, M. L. Adsorption Character for Removal Cu(II) by Magnetic Cu(II) Ion Imprinted Composite Adsorbent. *J. Hazard. Mater.* **2008**, *158*, 14−22.
(15) Liu, Y. Y.; Tang, J.; Chen, X. Q.; Xin, J. H. Decoration of Carbon Nanotubes with Chitosan. *Carbon* **2005**, *43*, 3178−3180.
(16) Wang, S.; Zhai, Y. Y.; Gao, Q.; Luo, W. J.; Xia, H.; Zhou, C. G. Highly Efficient Removal of Acid Red 18 from Aqueous Solution by Magnetically Retrievable Chitosan/Carbon Nanotube: Batch Study, Isotherms, Kinetics, and Thermodynamics. *J. Chem. Eng. Data* **2014**, *59*, 39−51.
(17) Yu, B. F.; Gao, Q.; Zhang, B.; Meng, X. Z.; Chen, Z. Review on Research of Room Temperature Magnetic Refrigeration. *Int. J. Refrig.* **2003**, *26*, 622−636.
(18) Aghayan, H.; Khanchi, A. R.; Mahjoub, A. R. Synthesis and Characterization of Cesium Molybdo Vanado Phosphate Immobilized on Platelet SBA-15: An Efficient Inorganic Composite Ion-exchanger for Gadolinium Ion Sorption. *Appl. Surf. Sci.* **2013**, *274*, 7−14.
(19) Liu, Y. J.; Zhang, Na. Gadolinium Loaded Nanoparticles in Theranostic Magnetic Resonance Imaging. *Biomaterials* **2012**, *33*, 5363−5375.
(20) Sherry, A. D.; Caravan, P.; Lenkinski, R. E. Primer on Gadolinium Chemistry. *J. Magn. Reson. Imaging* **2009**, *30*, 1240−1248.
(21) Stöber, W.; Fink, A.; Bohn, E. Controlled Growth of Monodisperse Silica Spheres in the Micro Size Range. *J. Colloid Interface Sci.* **1968**, *26*, 62−69.
(22) Wang, S.; Gao, Q.; Luo, W. J.; Xu, J.; Zhou, C. G.; Xia, H. Removal of Methyl Blue from Aqueous Solution by Magnetic Carbon Nanotube. *Water Sci. Technol.* **2013**, *68*, 665−673.
(23) Watts, P. C. P.; Mureau, N.; Tang, Z. N.; Miyajima, Y.; Carey, J. D.; Silva, S. R. The Importance of Oxygen-containing Defects on Carbon Nanotubes for the Detection of Polar and Non-polar Vapours through Hydrogen Bond Formation. *Nanotechnology* **2007**, *18*, 175701−175706.
(24) Corazzari, I.; Nisticò, R.; Turci, F.; Faga, M. G.; Franzoso, F.; Tabasso, S.; Magnacca, G. Advanced Physico−Chemical Charaterization of Chitosan by Means of TGA Coupled On-line with FTIR and GCMS: Thermal Degradation and Water Adsorption Capacity. *Polym. Degrad. Stab.* **2015**, *112*, 1−9.
(25) Cui, L.; Xiong, Z. H.; Guo, Y.; Liu, Y.; Zhao, J. C.; Zhang, C. J.; Zhu, P. Fabrication of Interpenetrating Polymer Network Chitosan/Gelatin Porous Materials and Study on Dye Adsorption Properties. *Carbohydr. Polym.* **2015**, *132*, 330−337.
(26) Williams, P. T.; Reed, A. R. Development of Activated Carbon Pore Structure via Physical and Chemical Activation of Biomass Fibre Waste. *Biomass Bioenergy* **2006**, *30*, 144−152.
(27) Yao, M. Z.; Joly, A. G.; Chen, W. Formation and Luminescence Phenomena of LaF_3:Ce^{3+} Nanoparticles and Lanthanide−Organic Compounds in Dimethyl Sulfoxide. *J. Phys. Chem. C* **2010**, *114*, 826−831.
(28) Rana, A.; Thakur, O. P.; Kumar, V. Effect of Gd^{3+} Substitution on Dielectric Properties of Nano Cobalt Ferrite. *Mater. Lett.* **2011**, *65*, 3191−3192.
(29) Zou, X. H.; Pan, J. M.; Ou, H. X.; Wang, X.; Guan, W.; Li, C. X.; Yan, Y. S.; Duan, Y. Q. Adsorptive Removal of Cr(III) and Fe(III) from Aqueous Solution by Chitosan/Attapulgite Composites: Equilibrium, Thermodynamics and Kinetics. *Chem. Eng. J.* **2011**, *167*, 112−121.
(30) Özcan, A. S.; Gök, Ö.; Özcan, A. Adsorption of Lead(II) Ions onto 8-Hydroxy Quinoline-immobilized Bentonite. *J. Hazard. Mater.* **2009**, *161*, 499−509.
(31) Zhou, Y. T.; Branford-White, C.; Nie, H. L.; Zhu, L. M. Adsorption Mechanism of Cu2+ from Aqueous Solution by Chitosan-coated Magnetic Nanoparticles Modified with α-Ketoglutaric Acid. *Colloids Surf., B* **2009**, *74*, 244−252.
(32) Luo, W. J.; Gao, Q.; Wu, X. L.; Zhou, C. G. Removal of Cationic Dye (Methylene Blue) from Aqueous Solution by Humic Acid-Modified Expanded Perlite: Experiment and Theory. *Sep. Sci. Technol.* **2014**, *49*, 2400−2411.
(33) Sun, Y. B.; Wang, Q.; Chen, C. L.; Tan, X. L.; Wang, X. K. Interaction Between Eu(III) and Graphene Oxide Nanosheets Investigated by Batch and Extended X-ray Absorption Fine Structure Spectroscopy and by Modeling Techniques. *Environ. Sci. Technol.* **2012**, *46*, 6020−6027.
(34) Li, Y. H.; Di, Z. C.; Ding, J.; Wu, D. H.; Luan, Z. K.; Zhu, Y. Q. Adsorption Thermodynamic, Kinetic and Desorption Studies of Pb^{2+} on Carbon Nanotubes. *Water Res.* **2005**, *39*, 605−609.
(35) Mou, F. Z.; Guan, J. G.; Ma, H. R.; Xu, L. L.; Shi, W. D. Magnetic Iron Oxide Chestnutlike Hierarchical Nanostructures: Preparation and Their Excellent Arsenic Removal Capabilities. *ACS Appl. Mater. Interfaces* **2012**, *4*, 3987−3993.
(36) Yang, S. B.; Han, C.; Wang, X. K.; Nagatsu, M. Characteristics of Cesium Ion Sorption from Aqueous Solution on Bentonite- and Carbon Nanotube-based Composites. *J. Hazard. Mater.* **2014**, *274*, 46−52.
(37) Bhatt, A. S.; Sakaria, P. L.; Vasudevan, M.; Pawar, R. R.; Sudheesh, N.; Bajaj, H. C.; Mody, H. M. Adsorption of an Anionic Dye from Aqueous Medium by Organoclays: Equilibrium Modeling, Kinetic and Thermodynamic Exploration. *RSC Adv.* **2012**, *2*, 8663−8671.
(38) Addo Ntim, S.; Mitra, S. Removal of Trace Arsenic to Meet Drinking Water Standards Using Iron Oxide Coated Multiwall Carbon Nanotubes. *J. Chem. Eng. Data* **2011**, *56*, 2077−2083.
(39) Garcia, R.; Pinel, C.; Madic, C.; Lemaire, M. Ionic Imprinting Effect in Gadolinium/Lanthanum Separation. *Tetrahedron Lett.* **1998**, *39*, 8651−8654.
(40) Liu, Y.; Liu, Z. C.; Gao, J.; Dai, J. D.; Han, J.; Wang, Y.; Xie, J. M.; Yan, Y. S. Selective Adsorption Behavior of Pb(II) by Mesoporous Silica SBA-15-supported Pb(II)-imprinted Polymer Based on Surface Molecularly Imprinting Technique. *J. Hazard. Mater.* **2011**, *186*, 197−205.
(41) Ren, Y. M.; Zhang, M. L.; Zhao, D. Synthesis and Properties of Magnetic Cu(II) Ion Imprinted Composite Adsorbent for Selective Removal of Copper. *Desalination* **2008**, *228*, 135−149.
(42) Liu, Y.; Tian, S. J.; Meng, X. G.; Dai, X. H.; Liu, Z. C.; Meng, M. J.; Han, J.; Wang, Y.; Chen, R.; Yan, Y. S.; Ni, L. Synthesis, Characterization, and Adsorption Properties of a Ce(III)-imprinted Polymer Supported by Mesoporous SBA-15 Matrix by a Surface Molecular Imprinting Technique. *Can. J. Chem.* **2014**, *92*, 257−266.
(43) Liu, B. J.; Lv, X.; Meng, X. H.; Yu, G. L.; Wang, D. F. Removal of Pb(II) from Aqueous Solution Using Dithiocarbamate Modified Chitosan Beads with Pb(II) as Imprinted Ions. *Chem. Eng. J.* **2013**, *220*, 412−419.
(44) Song, X.; Li, C.; Xu, R.; Wang, K. Molecular-ion-imprinted Chitosan Hydrogels for the Selective Adsorption of Silver (I) in Aqueous Solution. *Ind. Eng. Chem. Res.* **2012**, *51*, 11261−11265.
(45) Vigneau, O.; Pinel, C.; Lemaire, M. Ionic Imprinted Resins Based on EDTA and DTPA Derivatives for Lanthanides (III) Separation. *Anal. Chim. Acta* **2001**, *435*, 75−82.
(46) Liu, J.; Yang, X. L.; Cheng, X. Z.; Peng, Y.; Chen, H. M. Synthesis and Application of Ion-imprinted Polymer Particles for Solid-phase Extraction and Determination of Trace Scandium by ICP-MS in Different Matrices. *Anal. Methods* **2013**, *5*, 1811−1817.
(47) Lai, X. Q.; Hu, Y. L.; Fu, Y. Q.; Wang, L. L.; Xiong, J. Y. Synthesis and Characterization of Lu(III) Ion Imprinted Polymer. *J. Inorg. Organomet. Polym. Mater.* **2012**, *22*, 112−118.

DOI: 10.1021/acsami.5b07560
ACS Appl. Mater. Interfaces 2015, 7, 21047−21055